Structural Engineering and Mechanics, Vol. 16, No. 2 (2003) 127-139 127
DOI: http://dx.doi.org/10.12989/sem.2003.16.2.127

Analytical model for hybrid RC frame-steel wall systems

Y. L. Mo†

Department of Civil and Environmental Engineering, University of Houston, Houston, Texas, USA

S. F. Perng‡

Department of Civil Engineering, National Kaohsiung University of Applied Sciences, Kaohsiung, Taiwan

(Received July 3, 2002, Accepted May 7, 2003)

Abstract. Reinforced concrete buildings with shearwalls are very efficient to resist earthquake disturbances. In general, reinforced concrete frames are governed by flexure and shearwalls are governed by shear. If a structure included both frames and shearwalls, it is generally governed by shearwalls. However, the ductility of ordinary reinforced concrete is very limited. To improve the ductility, a series of tests on framed shearwalls made of corrugated steel was performed previously and the experimental results were compared with ordinary reinforced concrete frames and shearwalls. It was found that ductility of framed shearwalls could be greatly improved if the thickness of the corrugated steel wall is appropriate to the surrounding reinforced concrete frame. In this paper, an analytical model is developed to predict the horizontal load-displacement relationship of hybrid reinforced concrete frame-steel wall systems according to the analogy of truss models. This analytical model is based on equilibrium and compatibility conditions as well as constitutive laws of corrugated steel. The analytical predictions are compared with the results of tests reported in the previous paper. It is found that proposed analytical model can predict the test results with acceptable accuracy.

Key words: hybrid system; frame-wall interaction; corrugated steel plate; constitutive model; shear wall.

1. Introduction

Earthquake damages of buildings and the current design criteria show that a reinforced concrete shearwall is one of the best earthquake resistant elements for buildings (Fintel 1995), as it has high strength and rigidity. However, it collapses suddenly in a brittle manner. In other words, it is not so deformable to follow a large story drift of a high-rise building. High-rise buildings are so flexible that their story drift is not so small. If an ordinary reinforced concrete shearwall is installed in frames of high-rise building, dynamic response analysis has revealed that it first withstands earthquake forces but collapses before frames start to work. So it is desirable that the structural system of a high-rise building is firstly ductile against earthquakes, but secondly rigid and stiff

† Professor
‡ Assistant Professor

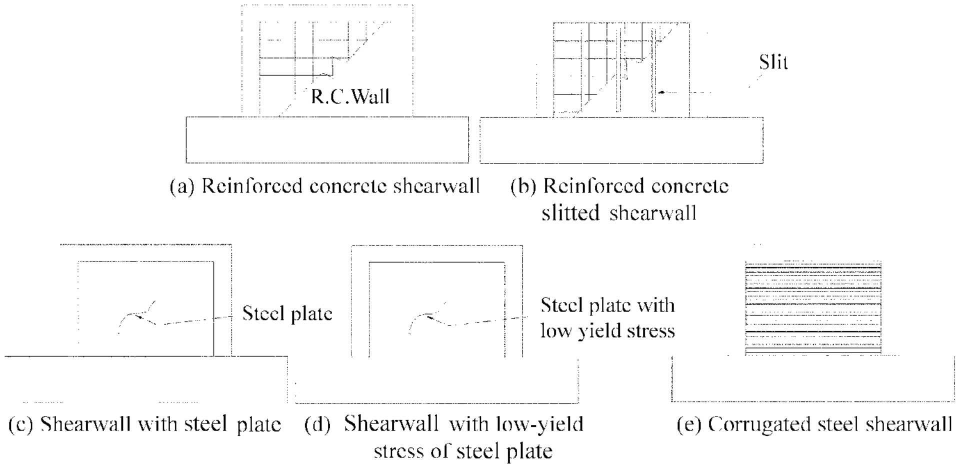

Fig. 1 Evolution of shearwalls

against frequent wind forces for the sake of occupants' comfort. If a ductile shearwall is developed and practically applicable, the safety of structures will be improved.

To improve the ductility of reinforced concrete shearwalls (Fig. 1a), Mo and Shiau (1993) tried to use low yield stress of rebars and high strength concrete as well as low reinforcement ratio. Since the ductility improvement made by Mo and Shiau (1993) is limited, Ohmori (1993) proposed slitted shearwalls. The slitted shearwall has vertical slits at certain intervals at mid-height of a wall (Fig. 1b). Hence, not only concrete but also reinforcement are absolutely cut by slitting materials. The slender parts between slits are named separated zone, which behave as a series of flexural short columns. Although slitted shearwalls have greater ductility, the construction of such walls takes longer time. Recently Lee and Yoo (1998) used steel plates to resist the shear force in the girder web. Driver *et al.* (1998) studied steel plate shearwalls (Fig. 1c). However, stiffeners need to be added to steel plate: to avoid adding stiffeners, Kitamura *et al.* (1995) applied low yield stress of steel to shearwalls (Fig. 1d). It should be noted that the steel plates used in Figs. 1(c) and 1(d) are generally considered isotropic.

Recently, the corrugated steel shearwalls installed in reinforced concrete frames were reported (Fig. 1e). The presence of corrugation, directional folding, indicates the corrugated steel plates to behave in an orthotropic manner. The seismic behavior of such shearwalls was experimentally investigated. The horizontal force-displacement relationship of such shearwalls was compared to that of each of ordinary reinforced concrete shearwalls and frame. It was found that the ductility of shearwalls made of corrugated steel is much greater than that of ordinary reinforced concrete shearwalls. The application of corrugated steel plates to resist shear was also proposed in Europe (Combault *et al*. 1993, Koenig *et al*. 1994), Asia (Yoda and Ohura 1993, Kondo *et al*. 1994) and North America (Mo *et al*. 2000, 2003, Hassanain 2001).

In this paper, an analytical model is developed to predict the horizontal load-displacement relationship of hybrid reinforced concrete frame-steel wall systems according to the analogy of truss models. This analytical model is based on equilibrium and compatibility conditions as well as constitutive laws of corrugated steel. The analytical predictions are compared with the results of tests reported in the previous paper (Masayasu *et al.* 1994). It is found that the proposed analytical model can predict the test results with acceptable accuracy.

2. Fundamental properties of corrugated steel

The tensile strength of a plain steel plate is similar to that of reinforcing bars. When the plain steel plate is subjected to compression, its compressive strength is governed by the plate stability. In other words, the compressive strength depends on the buckling strength. The corrugated steel plate is used in this study, and its geometric shape is wave-like shape that affects not only the axial deformation, but also the structural properties. From the viewpoint of the composites, corrugated steel plates are assumed to be orthotropic materials. The material properties of corrugated steel plates in both principal axes are interrelated that depend on wave height, plate thickness and wave shape, etc.

2.1 Modulus of elasticity

According to the study of Masayasu *et al*. (1994), the moduli of elasticity in the principal axes can be expressed with the following equations:

$$E_l = \alpha_s E_t (t/h)^2 \tag{1}$$

where E_l = Young's modulus of corrugated steel plate in the longitudinal direction
E_t = Young's modulus of corrugated steel plate in the transverse direction
h = wave height of corrugated steel plate
t = thickness of corrugated steel plate
α_s = shape coefficient of corrugated steel plate

Table 1 α_s for the corrugated steel plates

Type	wave-like shape	α_s
A	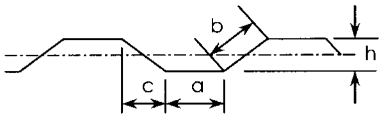	$\frac{a+c}{3a+b}$
B	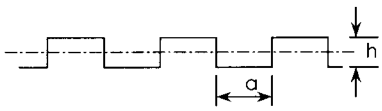	$\frac{a}{3a+h}$
C	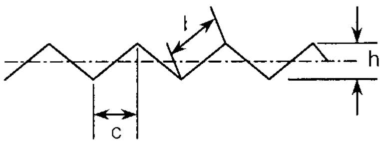	$\frac{c}{h}$
D	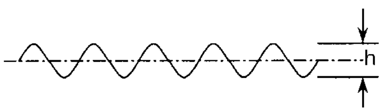	$\frac{4}{3\pi} = 0.424$

The α_s for the corrugated steel plates in this study can be expressed by the equation:

$$\alpha_s = \frac{a + c}{3a + b} \tag{2}$$

where parameters *a*, *b*, *c* are shown in Table 1.

2.2 Local and global buckling

According to the studies presented in the SSRC Guide edited by Galambos (1988), the buckling strength of corrugated steel plates is greater than that of plain steel plates. Basically, there are two models to calculate the buckling strength, namely, local and global buckling.

2.2.1 Local buckling

Elastic Buckling:

$$\tau_{cre} = k_s \frac{\pi^2 E}{12(1 - u^2)\left(\frac{w}{t}\right)^2} < 0.8\tau_y \tag{3}$$

Inelastic Buckling:

$$\tau_{cri} = (0.8\tau_{cre}\tau_y)^{0.5} < \tau_y \tag{4}$$

where

τ_{cre} = Elastic buckling strength.
τ_{cri} = Inelastic buckling strength.
h = Length in the long side of corrugated steel plate.
t = Thickness of corrugated steel plate.
w = Maximum length in the short side of corrugated steel plate.
E = Young's modulus of steel plate.
μ = Poisson's ratio.
k_s = Buckling coefficient.
τ_y = $f_y / \sqrt{3}$.
f_y = Yield stress of steel plate.

2.2.2 Global buckling

Elastic Buckling

$$\tau_{cre} = k_s \frac{D_y^{0.25} D_x^{0.75}}{th^2} < 0.8\tau_y \tag{5}$$

Otherwise, inelastic buckling will occur.

$$\tau_{cri} = (0.8\tau_{cre}\tau_y)^{0.5} \le \tau_y \tag{6}$$

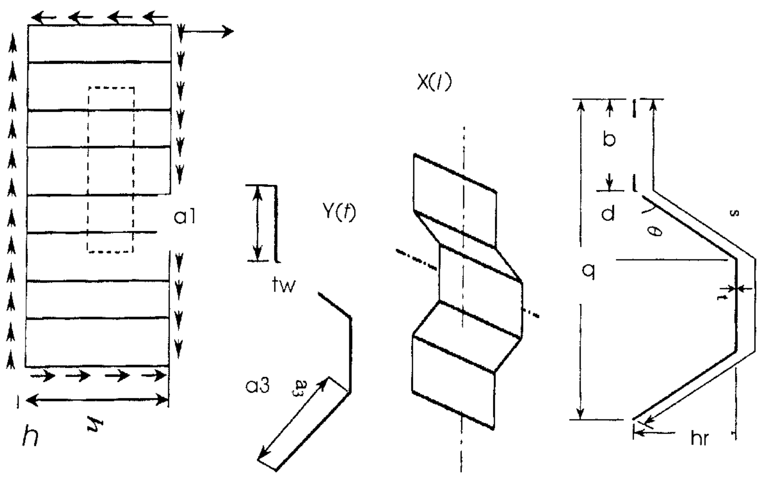

Fig. 2 Dimensions of corrugated steel plate

where

$$D_y = \left(\frac{q}{s}\right)\frac{Et^3}{12}$$

$$D_x = \frac{EI_x}{q}$$

$$I_s = 2bt\left(\frac{h_r}{2}\right)^2 + \frac{th_r^3}{6\sin\theta}$$

k_s = Coefficient depending on the boundary conditions and the aspect ratio of plate elements.
t = Thickness of corrugated steel plate.
h = Length in the long side of corrugated steel plate.
b, q, s, θ = Parameters shown in Fig. 2.
τ_t = $f_y/\sqrt{3}$.
E = Young's modulus of steel plate.
f_y = Yield stress of steel plate.

3. Analytical model

In the analytical model, the following assumptions are made.

1. Before buckling both compression and tension struts of corrugated steel plates are active simultaneously.
2. After buckling only tension struts are active and compression struts will lose their function.

Therefore, before and after buckling the structural behaviors of corrugated steel plates are different, resulting in different algorithm for analysis.

Before buckling, the buckling strengths predicted by Eqs. (1) to (6) need to be calculated, and the smallest strength is the governing value for buckling.

After buckling the truss model theory is employed, and is explained below.

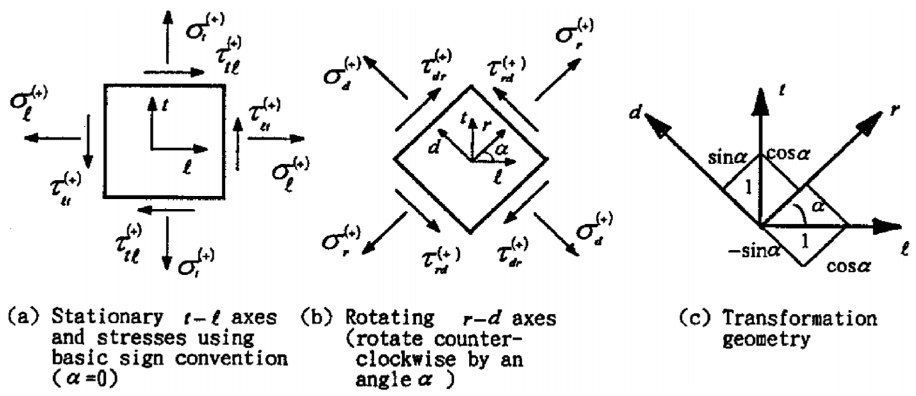

Fig. 3 Transformation of stress

3.1 Principle of transformation

As mentioned previously, the corrugated steel plates are considered orthotropic. The stress state in the principal directions can, therefore, be obtained by the transformation matrix, as proposed by Hsu (1993) for the stresses in a reinforced concrete membrane element. Fig. 3(a) shows a corrugated steel element in the stationary $l - t$ coordinate system, defined by the directions of the longitudinal and transverse steel. To find the three stress components in various directions, a rotating $d - r$ coordinate system is introduced in Fig. 3(b). The $d - r$ axes have been rotated counterclockwise by an angle of α with respect to the stationary $l - t$ axes. The three stress components in this rotating coordinate system are σ_d, σ_r, and τ_{dr} (or τ_{rd}). The relationship between the rotating stress components σ_d, σ_r, and τ_{dr} and the stationary stress components σ_l, σ_t, and τ_{lt} is the stress transformation. The relationship is a function of the angle α.

The relationship between the rotating $d-r$ axes and the stationary $l-t$ axes is shown by the transformation geometry in Fig. 3(c). A positive unit length on the l axis will have projections of $\cos\alpha$ and $-\sin\alpha$ and the d and r axes, respectively. A positive unit length on the t axis should give projections of $\sin\alpha$ and $\cos\alpha$. Hence, the rotation matrix $[R]$ is

$$[R] = \begin{bmatrix} \cos\alpha & \sin\alpha \\ -\sin\alpha & \cos\alpha \end{bmatrix} \tag{7}$$

The relationship between the stresses in the $l-t$ coordinate $[\sigma_{dr}]$ is

$$[\sigma_{lt}] = [R]^T[\sigma_{dr}][R] \tag{8}$$

where

$$[\sigma_{lt}] = \begin{bmatrix} \sigma_l & \tau_{lt} \\ \tau_{lt} & \sigma_t \end{bmatrix} \tag{9}$$

$$[\sigma_{dr}] = \begin{bmatrix} \sigma_d & \tau_{dr} \\ \tau_{rd} & \sigma_r \end{bmatrix} \tag{10}$$

3.2 Equilibrium conditions

If the $d-r$ axes are defined as the principal axes, τ_{dr} must vanish. Introducing the reinforced concrete sign convention, and performing the matrix multiplications as well as noticing that $\tau_{lt} = \tau_{tl}$ and $\tau_{dr} = \tau_{rd}$ give the following equations when only the steel tension struts are considered.

$$\sigma_l = \sigma_d \cos^2\alpha + \sigma_r \sin^2\alpha \tag{11}$$

$$\sigma_t = \sigma_d \sin^2\alpha + \sigma_r \cos^2\alpha \tag{12}$$

$$\tau_{lt} = (-\sigma_d + \sigma_r)\sin\alpha\cos\alpha \tag{13}$$

3.3 Compatibility conditions

The same principle of transformation for stresses can be applied to strains. Therefore, the following compatibility equations can be derived (Hsu 1993).

$$\varepsilon_l = \varepsilon_d \cos^2\alpha + \varepsilon_r \sin^2\alpha - \gamma_{dr}\sin\alpha\cos\alpha \tag{14}$$

$$\varepsilon_t = \varepsilon_d \sin^2\alpha + \varepsilon_r \cos^2\alpha + \gamma_{dr}\sin\alpha\cos\alpha \tag{15}$$

$$\gamma_{lt} = 2(-\varepsilon_d + \varepsilon_r)\sin\alpha\cos\alpha + (\cos^2\alpha - \sin^2\alpha)\gamma_{dr} \tag{16}$$

3.4 Constitutive laws

According to the tension tests of corrugated steel plates, the stress-strain relationship can be expressed as follows:

$$f_s = \varepsilon_s E_s \quad \text{if} \quad \varepsilon_s \le \frac{f_y}{E_s} \tag{17a}$$

$$f_s = f_y + (f_1 - f_y)\frac{\varepsilon_s - \varepsilon_y}{\varepsilon_1 - \varepsilon_y} \quad \text{if} \quad \frac{f_y}{E_s} < \varepsilon_s < \varepsilon_1 \tag{17b}$$

$$f_s = f_1 \quad \text{if} \quad \varepsilon_1 < \varepsilon_s < \varepsilon_2 \tag{17c}$$

where

ε_s = steel strain

e_1 = 0.08, ε_2 = 0.215

f_s = steel strength

f_1 = maximum strength (490 N/mm^2), f_y = yield stress

E_s = Young's modulus

Using the Von-Mises yield criterion (Salmon and Johnson 1980), the shear yield stress is expressed by:

$$\tau_y = f_y / \sqrt{3} \tag{18}$$

Assuming the elastoplastic behavior for the shear stress-shear strain relationship of steel gives

$$\tau_{web} = \gamma_{web} G_{web} \qquad \text{if} \quad \gamma_{web} \le \frac{\tau_{weby}}{G_{web}} \tag{19a}$$

$$\tau_{web} = \tau_{weby} \qquad \text{if} \quad \gamma_{web} > \frac{\tau_{weby}}{G_{web}} \tag{19b}$$

where

γ_{web} = shear strain of steel plate.
τ_{web} = shear stress of steel plate.
τ_{weby} = yield shear stress of steel plate.
G_{web} = shear modulus of steel plate.

It is assumed that corrugated steel plates are orthotropic.
The stress and strain relationship in the $l-t$ axes can be expressed as

$$\begin{Bmatrix} \sigma_l \\ \sigma_t \\ \tau_{lt} \end{Bmatrix} = \begin{bmatrix} Q_{11} & Q_{12} & 0 \\ Q_{12} & Q_{22} & 0 \\ 0 & 0 & Q_{66} \end{bmatrix} \begin{Bmatrix} \varepsilon_l \\ \varepsilon_t \\ \gamma_{lt} \end{Bmatrix} \tag{20}$$

where

$$Q_{11} = S_{22}/(S_{11}S_{22} - S_{22}^2)$$
$$Q_{12} = -S_{12}/(S_{11}S_{22} - S_{22}^2)$$
$$Q_{22} = S_{11}/(S_{11}S - S_{22}^2)$$
$$Q_{66} = 1/(S_{66})$$
$$S_{11} = 1/E_t$$
$$S_{12} = -(v_{lt})/E_l$$
$$S_{22} = 1/E_t$$
$$S_{66} = 1/G_{lt}$$

Note that the Q_{11}, Q_{12}, Q_{22}, Q_{66}, and S_{11}, S_{12}, S_{22}, S_{66} are related. S_{11}, S_{12}, S_{22}, S_{66} are functions of Young's Moduli E_l and E_t.
Using the transformation matrix, the stress-strain relationship of corrugated steel plates in the $d-r$ axes (i.e. principal directions) can be expressed.

$$\begin{Bmatrix} \sigma_d \\ \sigma_r \\ \tau_{dr} \end{Bmatrix} = \begin{bmatrix} \overline{Q}_{11} & \overline{Q}_{12} & \overline{Q}_{16} \\ \overline{Q}_{12} & \overline{Q}_{22} & \overline{Q}_{26} \\ \overline{Q}_{16} & \overline{Q}_{26} & \overline{Q}_{66} \end{bmatrix} \begin{Bmatrix} \varepsilon_d \\ \varepsilon_r \\ \gamma_{dr} \end{Bmatrix} \tag{21}$$

where

$$\bar{Q}_{11} = Q_{11}\cos^4\alpha + 2(Q_{12} + 2Q_{66})\sin^2\alpha\cos^2\alpha + Q_{22}\sin^4\alpha$$

$$\bar{Q}_{12} = (Q_{11} + Q_{22} - 4Q_{66})\sin^2\alpha\cos^2\alpha + Q_{12}(\cos^4\alpha + \sin^4\alpha)$$

$$\bar{Q}_{22} = Q_{11}\sin^4\alpha + 2(Q_{12} + 2Q_{66})\sin^2\alpha\cos^2\alpha + Q_{22}\cos^4\alpha$$

$$\bar{Q}_{16} = (Q_{11} - Q_{12} - 2Q_{66})\sin\alpha\cos^3\alpha + (Q_{12} - Q_{22} + 2Q_{66})\sin^3\alpha\cos\alpha$$

$$\bar{Q}_{26} = (Q_{11} - Q_{12} - 2Q_{66})\sin^3\alpha\cos\alpha + (Q_{12} - Q_{22} + 2Q_{66})\sin\alpha\cos^3\alpha$$

$$\bar{Q}_{66} = (Q_{11} + Q_{12} - 2Q_{12} - 2Q_{66})\sin^2\alpha\cos^2\alpha + Q_{66}(\cos^4\alpha + \sin^4\alpha)$$

It is assumed in this paper that $d - r$ axes are the principal stress axes. In the condition of post-buckling, $\tau_{dr} = 0$, $\sigma_d = 0$. Eq. (21) becomes

$$\begin{Bmatrix} 0 \\ \sigma_r \\ 0 \end{Bmatrix} = \begin{bmatrix} \bar{Q}_{11} & \bar{Q}_{12} & \bar{Q}_{16} \\ \bar{Q}_{12} & \bar{Q}_{22} & \bar{Q}_{26} \\ \bar{Q}_{16} & \bar{Q}_{26} & \bar{Q}_{66} \end{bmatrix} \begin{Bmatrix} \varepsilon_d \\ \varepsilon_r \\ \gamma_{dr} \end{Bmatrix} \tag{22}$$

4. Solution algorithm

In the low-rise frame-wall systems, the wall is restrained by the boundary beam and column elements to resist the horizontal shear force. Therefore, it is assumed that $\varepsilon_t = 0$, $\varepsilon_l = 0$. Substituting $\varepsilon_t = 0$ and $\varepsilon_l = 0$ into Eq. (14) and Eq. (15), respectively, and adding these two equations give

$$\varepsilon_d = -\varepsilon_r \tag{23}$$

After the buckling of the wall, σ_r will not be affected by ε_d. Hence, substituting $\bar{Q}_{11} = \bar{Q}_{12} = \bar{Q}_{16} = 0$ into Eq. (22) gives

$$\begin{Bmatrix} 0 \\ \sigma_r \\ 0 \end{Bmatrix} = \begin{bmatrix} 0 & 0 & 0 \\ 0 & \bar{Q}_{22} & \bar{Q}_{26} \\ 0 & \bar{Q}_{26} & \bar{Q}_{66} \end{bmatrix} \begin{Bmatrix} \varepsilon_d \\ \varepsilon_r \\ \gamma_{dr} \end{Bmatrix} \tag{24}$$

i.e.

$$\gamma_{dr} = -\frac{\bar{Q}_{26}}{\bar{Q}_{66}}\varepsilon_r \tag{25}$$

$$\sigma_r = \left(Q_{22} - \frac{Q_{26}^2}{Q_{66}}\right)\varepsilon_r \tag{26}$$

Substituting Eq. (23) and Eq. (25) into Eq. (14) with $\varepsilon_l = 0$ gives

$$(-\varepsilon_r)\cos^2\theta + \varepsilon_r \sin^2\alpha + \left(\frac{\overline{Q}_{26}^2}{\overline{Q}_{66}}\varepsilon_r\right)\sin\alpha\cos\alpha = 0 \tag{27}$$

Eq. (27) divided by $\varepsilon_r \sin\alpha\cos\alpha$, gives

$$-\cot\alpha + \tan\alpha + \frac{\overline{Q}_{26}}{\overline{Q}_{66}} = 0 \tag{28}$$

α can be determined from Eq. (28). The shear stress can be found by

$$\tau = \frac{V}{0.5*(bd)} \tag{29}$$

where
V = Shear force.
b = Wall width.
d = Effective length of wall

$$\tau = \tau_{lt} = (\tau_r - \tau_d)\sin\alpha\cos\alpha \tag{30}$$

The horizontal displacement at the top of the wall is

$$\delta = \gamma H \tag{31}$$

where
H = Wall height

$$\gamma = \gamma_{lt} = 2*(\varepsilon_r - \varepsilon_d)\sin\alpha\cos\alpha \tag{32}$$

Based on the equilibrium and compatibility conditions as well as constitutive laws derived above, the primary curve of corrugated steel plates can be determined by the following steps.

1. Before buckling, the buckling stress and the corresponding shear strain and the shear stress can be calculated by Eqs. (1)-(6) and Eq. (19). The shear force and the corresponding horizontal displacement are calculated by Eqs. (29) and (31).
2. After buckling, use Eq. (28) to find α.
3. Select a ε_r, calculate γ_{dr} and σ_r by Eqs. (25) and (26). Check if σ_r reaches yield stress. If yes, $\sigma_r = f_y$.
4. Use Eq. (13) to find τ_{lt}, check if τ_{lt} reaches τ_y. If yes, $\tau_{lt} = \tau_y = \frac{f_y}{\sqrt{3}}$, and $V = \tau bd/2$.
5. Use Eq. (16) to calculate γ, and $\delta = \gamma H$.
6. Select a new ε_r, repeat steps 3 to 5 until ε_r reaches its ultimate strain of 0.215.

5. Comparison of theory with tests

Five hybrid RC frame-corrugated steel wall specimens were tested under reversed cyclic loads previously reported (Mo and Perng 2000). The dimensions and material properties of these specimens were reported by Perng (2000). These test results are employed to verify the proposed analytical model. Fig. 4 indicates the test data and the analytical results for all five specimens. There

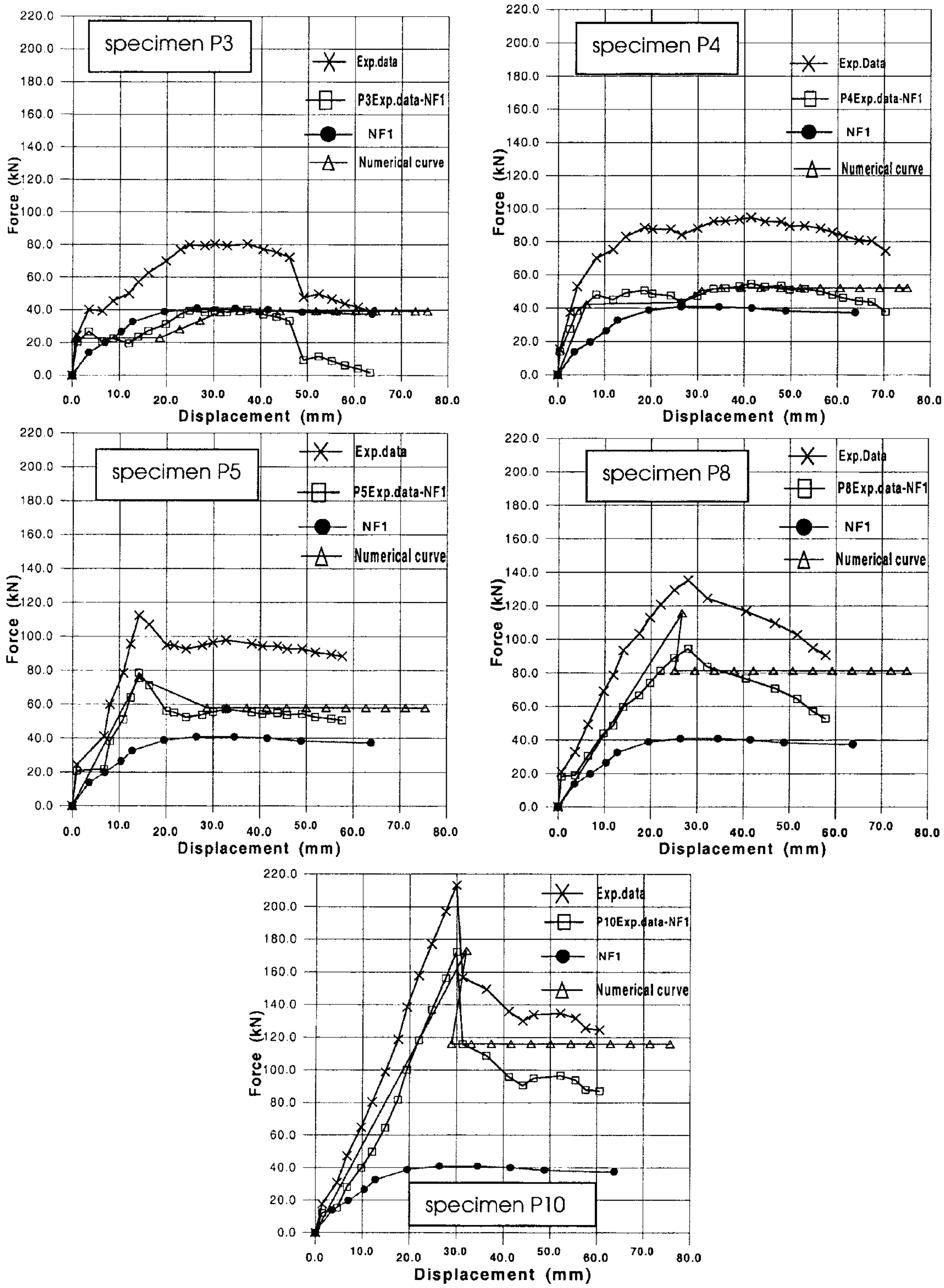

Fig. 4 Theoretical Primary curves compared with tests

are four curves in each figure. The curve with crosses is the experimental horizontal force-displacement relationship for the hybrid RC frame-steel wall system. The curve with solid circles is the horizontal force-displacement relationship for the pure RC frame (Specimen NF1) that was also experimentally investigated. The curve with hollow rectangles is the horizontal force-displacement relationship for the corrugated steel wall only that is obtained by using the results for the hybrid RC frame-steel wall subtracted by those for the pure RC frame. The curve with hollow triangles is the analytical results for the corrugated steel wall. The following observations can be made from Fig. 4.

1. The difference between the analytical and experimental maximum forces is less than 5% for all specimens.
2. When the thickness of corrugated steel plates is small, such as: specimens P3, P4, P5, the predicted results are in good agreement with the test data throughout the loading history.
3. When the thickness of corrugated steel plates is greater, such as specimens P8 and P10, the predicted results are also in good agreement with the test data except the descending branch.
4. The reason for the discrepancy between the test data and the analytical results in the descending branch can be explained below. When the thickness of corrugated steel plates is greater (such as specimen P8 and P10), the failure of the corrugated steel plates becomes brittle. Hence, it is not in the range of concern for practice. It should be noted that in the proposed analytical model the elastoplastic behavior of corrugated steel plates indicates an approximate horizontal line in the descending branch.

6. Conclusions

Based on equilibrium and compatibility conditions as well as constitutive laws of corrugated steel plates, an analytical model is presented to predict the force-displacement relationship of corrugated steel walls. When the analytical results are compared to the test date reported previously, it is found that the analytical model can predict the behavior of corrugated steel walls with acceptable accuracy throughout the loading history in the cases of smaller thickness of corrugated steel plates; in contrast, in the cases with greater thickness of corrugated steel plates the analytical model may be improved in the descending portion of the force-displacement relationship of corrugated steel walls in the future. It should be noted that since the failure mode of the cases with greater thickness of corrugated steel plates is brittle, it is not in the concern of practice.

References

Combault, J., Lebon, J.D. and Pei, G. (1993), "Box-girders using corrugated steel webs and balanced cantilever construction", *FIP Symposium*, Kyoto, Japan, October 17-20, 417-424.

Driver, R.G., Kulak, G.L., Kennedy, D.J.L. and Eliwi, A.E. (1998), "Cyclic test of four-story steel plate shear wall", *J. Struct. Eng.*, ASCE, **124**(2), February, 112-120.

Fintel, M. (1995), "Performance of building with shear walls in earthquakes of the last thirty years", *PCI Journal*, **40**(3), 62-80.

Galambos, T.V. (1988), *Guide to Stability Design Criteria for Metal Structure*, John Wiley & Sons, Inc., New York.

Hassanain, M.A. (2001), "Prestressed composite bridges with high-performance concrete decks and high-performance steel corrugated webs", *Proc. of the Fifth National Workshop on Bridge Research in Progress*, Minneapolis, Minnesota, October 8-10, 307-312.

Hsu, T.T.C. (1993), *Unified Theory of Reinforced Concrete*, CRC Press, Boca Raton, Florida, 150.

Kitamura, H., Teramoto, T., Kihara, H., Torri, S., Iwata, M., Fujisawa, K., Shimizu, T. and Nakagawa, S. (1995), "Application of high-rise buildings with low yield strength steel wall", *Symposium on a New Direction in Seismic Designs*, Tokyo, Japan.

Kondo, M., Shimizu, Y., Kobayashi, K. and Hattori, M. (1994), "Design and construction of the Shinkai Bridge-prestressed concrete bridge using corrugated steel webs", (in Japanese), *Bridge and Foundation*, September, 13-20.

König, G., Duda, H. and Zink, M. (1994), "Neue Entwicklungen im Spannbetonbrückenbau", (in German), *New Developments in Prestressed Concrete Bridges*, Beton-und Stahlbetonbau, **89**(4), 85-89.

Lee, S.C. and Yoo, C.H. (1998), "Strength of plate girder web panels under pure shear", *J. Struct. Eng.*, ASCE, **124**(2), February, 184-194.

Masayasu, K., Yoichi, S., Kinishi, K. and Masaaki, H. (1994), "Design and construction of the Shinkai Bridge prestressed concrete bridges using corrugated steel webs", (in Japanese), *Bridge and Fondation*, 13-20, September.

Mo, Y.L., Jeng, C.H. and Chang, Y.S. (2000), "Torsional behavior of prestressed concrete box-girder bridges with corrugated steel webs", *ACI Struct. J.*, **97**(6), Nov.-Dec., 849-859.

Mo, Y.L., Jeng, C.H. and Krawinkler, H. (2002), "Experimental and analytical studies of innovative prestressed concrete box-girder bridges", *Materials and Structures*, RILEM, **36**, March, 99-107.

Mo, Y.L. and Perng, S.F. (2000), "Hybrid RC frame-steel wall systems", SP-196, *Composite and Hybrid Systems*, ACI, 189-213.

Mo, Y.L. and Shiau, W.C. (1993), "Ductility of low-rise structural walls", *Magazine of Concrete Research*, **45**(163), 131-138.

Ohmori, N. (1993), "Development of slitted shear walls", *Earthquake Resistance of Reinforced Concrete Structures*, A Volume Honoring Hiroyuki Aoyama, Editor: Okada, T., Department of Architecture, Faculty of Engineering, University of Tokyo Press, November 25.

Perng, S.F. (2000), "Behavior of framed shearwalls with corrugated steel", Ph.D. Dissertation, Department of Civil Engineering, National Cheng Kung University, Tainan, Taiwan, April.

Salmon, C.G. and Johnson, J.E. (1980), *Steel Structures*, Second Edition, Harper & Row Publishers, New York, N.Y.

Yoda, T. and Ohura, T. (1993), "Torsional behavior of composite PC box girders with corrugated steel webs", *Japanese Society of Civil Engineers*, **39A**, March, 1251-1258.